J. Fluid Mech. (1976), *vol.* 75, *part* 2, *pp.* 257–271
Printed in Great Britain

Vortex shedding from a cylinder vibrating in line with an incident uniform flow

By OWEN M. GRIFFIN AND STEVEN E. RAMBERG
Naval Research Laboratory, Washington, D.C. 20375

(Received 29 September 1975)

A study has been made of the wake of a cylinder vibrating in line with an incident steady flow. The Reynolds number for the experiments was 190, and the vortex shedding was at all times synchronized with the vibrations of the cylinder, which were in a range of frequencies near twice the Strouhal shedding frequency for the stationary cylinder. Two distinct vortex wake patterns were encountered. The first is a complex regime in which two vortices are shed during each cycle of the vibration and form an alternating pattern of vortex pairs downstream. The second pattern is an alternating street which results from the shedding of a single vortex during each cycle of the cylinder's motion. The street geometry in the latter case shares many basic characteristics with the wake of a cylinder vibrating in cross-flow. These include the effects of vibration amplitude and frequency on the longitudinal and transverse spacing of the vortices. The results obtained from these experiments in air are in agreement with previous findings from free- and forced-vibration experiments in water at both higher and lower Reynolds numbers.

1. Introduction

When one of the natural frequencies of a bluff body is near the Strouhal frequency at which vortices are naturally shed, the body can undergo vortex-induced oscillations in a direction transverse to the incident flow if the damping of the system is sufficiently small. A range of frequencies also exists near the Strouhal frequency of vortex shedding where forced transverse vibrations of the body cause the vortex frequency to be captured by, or to synchronize with, the body's vibration frequency. The body and the wake then have the same characteristic frequency and the Strouhal frequency of vortex shedding is suppressed in favour of a single, synchronized frequency of vibration and vortex shedding.

Most recent investigations of vortex-induced oscillations and their forced-body analogues have concentrated upon vibrations transverse to the flow, but vortex-induced oscillations also occur in the direction in line with the incident flow. Oscillations parallel to the incident flow generally occur at frequencies near twice the Strouhal frequency, though some investigators have observed vortex-induced in-line oscillations to occur also at three to four times the Strouhal frequency. Not only do these in-line oscillations have practical consequences relating to the design of offshore and underwater structures, but from a fundamental standpoint the vortex-induced and forced in-line oscillations of bluff bodies also form an important and relatively unexplored class of oscillatory flows.

The purpose of this paper is to examine in an initial way the in-line vibrations of cylinders in the presence of an incident uniform flow. Bounds for the locked-on regime have been obtained from wind-tunnel measurements, and flow-visualization photographs have been taken in order to investigate the effects of in-line vibration amplitude and frequency on the vortex street behind the cylinder. Measurements of the vortex spacing in the wake have been made both from hot-wire surveys of the wake and directly from the photographic negatives. Finally, some comparisons are made with other recent in-line vibration experiments and between the effects on the vortex wake of in-line and transverse oscillations of the cylinder.

2. Related investigations

From a historical standpoint, studies of the vortex-induced oscillations of structures have largely dealt with the cross-flow, wind-induced oscillations of stacks and large towers, the cross-flow 'strumming' vibrations of marine cables, and wind-tunnel experiments on the flow around circular cylinders. Comprehensive and useful summaries of virtually all known aspects of the flow around stationary and vibrating cylinders have recently been made by Parkinson (1971), Mair & Maull (1971), King, Prosser & Johns (1973) and Berger & Wille (1972). The paper by Parkinson covered in general the wind-induced oscillation of structures while Mair & Maull reported on a Euromech symposium on vortex shedding. Berger & Wille reviewed the topic of oscillatory flows while emphasizing vortex wake phenomena and King *et al.* considered the flow fields around stationary and vibrating cylinders as they apply to the design of offshore pilings.

Usually, when vortex-induced oscillations are mentioned, one thinks of circular cylinders vibrating normal to an incident flow since, in air, the shedding of vortices produces periodic forces which act primarily in the cross-flow direction at a frequency near the Strouhal value for vortices of like sign. The in-line component of the periodic force, at twice the Strouhal frequency, is typically an order of magnitude less than the cross-flow component and, owing to the small density of air, does not excite the structure. With the increased use of lightly damped cylindrical structures in water, the problem of in-line oscillations has been increased because of the larger fluid forces in that medium and the lower velocities at which the in-line vibrations are initiated.

Investigation of the in-line oscillations of bluff cylinders began in earnest following the troublesome and sometimes damaging vortex-induced oscillations of pilings during the construction of an oil terminal on the Humber estuary in England during the later 1960s. A description of the problems encountered at the construction site has been given by Sainsbury & King (1971) and a discussion of subsequent full-scale experiments to ascertain the causes of the vibrations has been reported by Wootton *et al.* (1972). A readily accessible summary of the latter report appears in the proceedings of a recent symposium on flow-induced structural vibrations (Naudascher 1974).

A cylindrical bluff body is excited into cross-flow oscillations when the reduced velocity $U_r = U/f_n d \sim 5$. This critical velocity is the reciprocal of the Strouhal number ($St = f_s d/U \sim 0{\cdot}2$) evaluated at $f_s \sim f_n$, where f_n is a natural frequency of the body. It might be anticipated that in-line oscillations occur at $U_r = 2{\cdot}5$ since the frequency of the drag fluctuations is $2f_s$, or twice the Strouhal frequency. King (1974) and King *et al.* (1973) observed that the in-line oscillations occur over a range $U_r = 1{\cdot}5$–$4{\cdot}0$ and in two distinct resonant response regimes separated by $U_r = 2{\cdot}5$. The response in each of the two instability regions depends strongly on the non-dimensional parameter

$$k_S = 2m\delta/\rho d^2,$$

often called a 'reduced damping', which is the product of the logarithmic decrement of the damping and the ratio of the virtual mass to the displaced fluid mass. An analogous dependence for the cross-flow amplitudes of vortex-induced oscillation in both air and water is well known for a wide variety of bluff cylindrical structures (see Griffin, Skop & Ramberg 1975). The in-line oscillations reach peak amplitudes of only about $0{\cdot}25d$ peak to peak even at low damping values for the structure, whereas cross-flow amplitudes of oscillation are known to reach 2–$3d$ when the damping is small.

King *et al.* observed two distinct flow patterns for the two resonant regions of the in-line response. For $U_r < 2{\cdot}5$ the flow was characterized by the shedding of two vortices of opposite sign from opposite sides of the cylinder during each motion cycle, while for $U_r > 2{\cdot}5$ a single vortex was shed during each motion cycle and a street of alternately rotating vortices was formed downstream of the cylinder. Two such flow regimes had been postulated by Wootton *et al.* (1972) in trying to explain the appearance of two in-line instability regions during the full-scale field experiments at Immingham.

Recently, Tatsuno (1972) measured the locking-on boundaries and vortex spacing for a cylinder that was towed through still water and vibrated in line with the tow direction. Flow-visualization photographs were taken of the vortex streets generated over a range of frequencies both within and outside the locked-on regime at a Reynolds number of 100. Tanida, Okajima & Watanabe (1973) measured the lift and drag forces on circular cylinders that were towed through still water and forced to vibrate in line with and transverse to the tow direction. These experiments at Reynolds numbers of 80 and 4000 included not only measurements of the lift and drag forces, but also measurements of the range of the frequency-locking for both the cross-flow and the in-line motions of single cylinders.

3. Experimental systems and procedures

The experiments reported in this paper were performed in an open-jet wind tunnel which has been described in detail by Griffin & Votaw (1972) and Griffin (1971). The exit of the tunnel is 75×75 mm in area and is preceded by a 20:1

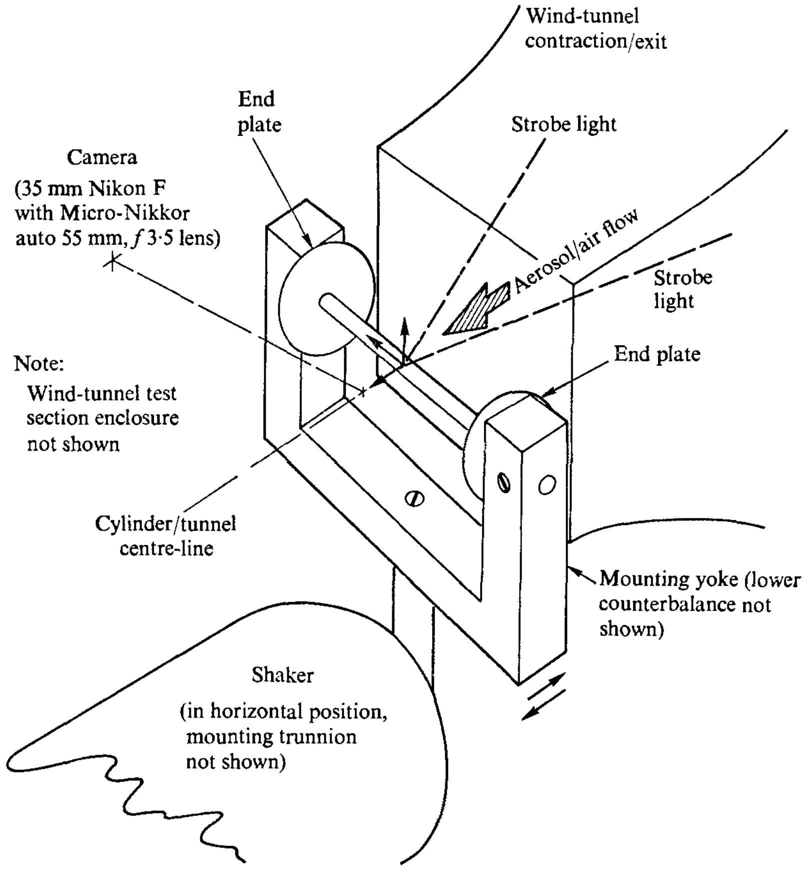

FIGURE 1. A line diagram of the experimental set-up. The distance 75 mm between the end plates is equal to the width of the tunnel exit. The centre of the camera lens was in the same horizontal plane as the cylinder axis, and the camera was focused on the centre-plane of the tunnel, about 3–4 diameters downstream from the cylinder.

contraction section. The photographs were taken by introducing into the wind tunnel an aerosol of submicron-sized particles of DOP, or di(2-ethylhexyl) phthalate, and complete descriptions of the flow-visualization set-up and procedures are available in a paper by Griffin *et al.* (1973).

The present experiments were performed with a smooth circular cylinder which was vibrated in line with the incident flow. This was accomplished by mounting the shaker used in previous cross-flow vibration experiments on a vibration-isolated trunnion which enabled it to be fixed at various angles from the vertical. The cylinder, 4 mm in diameter and fitted with sharp-edged end plates 38 mm in diameter, was fixed in a yoke assembly which executed translatory motion and resulted in sinusoidal oscillations of the cylinder in a horizontal plane just downstream of the tunnel exit when the shaker was rotated 90° from the vertical. A sketch of the experimental set-up is shown in figure 2.

Velocity measurements in the cylinder wake were made with DISA hot-wire anemometers (55D01) and low interference hot-wire probes (55F01), and the

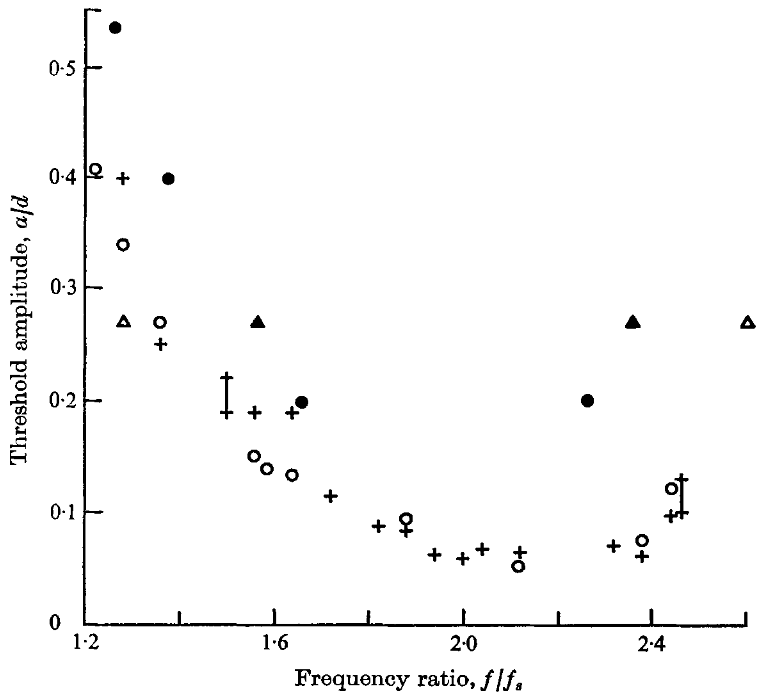

FIGURE 2. Amplitude and frequency regions over which the vibrations of a cylinder control the vortex shedding. Measurements of in-line oscillations near twice the Strouhal frequency ($f \approx 2f_s$). Present study, $Re = 190$: $+$, oscilloscope comparison; $\bigcirc$, spectral measurements, Tanida *et al.* (1973): $\blacktriangle$, $Re = 80$; $\triangle$, $Re = 4000$. Tatsuno (1972): $\bullet$, $Re = 100$.

velocity signal was carefully linearized in the speed range of interest with a DISA linearizer (55D10). In addition, an analog correlator (DISA 55D70) was available for measuring the longitudinal spacing of the vortices from a downstream correlogram of the vortex velocity signal and a reference signal obtained from the cylinder motion. A Honeywell-Saicor Model 51B Real-Time Spectrum Analyzer and Digital Averager, which provided both instantaneous and averaged spectra of the velocity and cylinder motion signals directly on the screen of an oscilloscope or on an x, y recorder, was used in the measurement of the bounds for the locked-on regime.

4. Bounds for the frequency-locking between the cylinder and its wake

All of the new experiments reported in this paper were performed at a Reynolds number $Re = 190$, since this particular flow speed gave a set of optimal conditions for simultaneously operating the flow-visualization apparatus and the wind tunnel. In addition, it makes possible a brief comparison with some earlier cross-flow vibration experiments (see Griffin & Ramberg 1974, 1975) that were reported for the same Reynolds number. The measured bounds of the locked-on regime for a cylinder which was vibrated in line with the flow are plotted in figure 2.

The regime over which the vortex frequency was controlled by the vibrations of the cylinder was determined by two methods. After adjusting the flow speed to achieve a Reynolds number of 190, the shedding frequency f_s of the stationary cylinder was measured with a hot-wire probe placed downstream in the separated shear layer behind the cylinder. The cylinder was then oscillated at various frequencies and amplitudes near twice the Strouhal frequency. At each frequency the amplitude of oscillation was increased until the vortex-shedding frequency became synchronized with the cylinder-motion signal on an oscilloscope. The minimum amplitude for wake capture is the threshold amplitude, and the results of these measurements are plotted in figure 2. A second method was also used to determine the range of the synchronization away from twice the Strouhal frequency. The hot-wire signal was fed into a real-time spectrum analyser and digital integrator which provided outputs of both the instantaneous and the averaged spectra of the velocity fluctuations. Again the amplitude was varied at each vibration frequency near $2f_s$ and the threshold amplitude for the locking-on was ascertained. The criterion employed was the absence in the velocity spectrum of a peak at the Strouhal frequency or double its value together with the emergence of a strong peak in the spectrum at the vibration frequency or half its value. The locking-on thresholds obtained by this method are also plotted in figure 2 and the results are in good agreement with those obtained from a comparison of oscilloscope signals.

The locked-on range for the in-line vibrations extends from about 120 % to nearly 250 % of the Strouhal frequency f_s, and this interval corresponds to a range of reduced velocities $U_r = U/f_n d$ from 2·1 to 4·4. This compares quite well with the range of reduced velocities $U_r = 1{\cdot}5$–$4{\cdot}0$ over which a flexible cantilevered circular cylinder was observed by King *et al.* (1973) and King (1974) to oscillate in line with an incident flow of water.

Some results obtained by Tatsuno (1972) are plotted in the figure for comparison. The locking-on boundaries measured by Tatsuno during experiments in water are in good agreement with the present results obtained in air at the higher Reynolds number. Also plotted in the figure are the results obtained by Tanida *et al.* (1973) when their cylinder was vibrated in line and towed through still water at Reynolds numbers of 80 and 4000. The agreement is again acceptable, especially at the frequencies less than twice the Strouhal frequency. In their experiments Tanida *et al.* investigated only a single vibration amplitude of 27 % of a diameter.

The results obtained in the present experiments show that the locking-on threshold is slightly lower in amplitude than in the corresponding cross-flow case (see Koopmann 1967; or Griffin & Ramberg 1974) and that it extends to lower relative frequencies $f/2f_s$. These findings are not surprising since vortex-induced in-line vibrations are initiated at lower vibration amplitudes and reach peak values which are lower by a substantial amount than the cross-flow amplitudes which can be reached by a similar bluff body. Also, as stated earlier, the locked-on frequency range for the present forced-body experiments compares well with available observations of vortex-induced in-line oscillations.

Frequency f (Hz)	Frequency ratio f/f_s	Amplitude of vibration a/d (peak to peak)
63·9	1·74	0·12
64·4	1·76	0·22
69·2	1·88	0·12
—	—	0·15
—	—	0·20
—	—	0·24
70·4	1·92	0·10
75·6	2·06	0·06
80·4	2·20	0·06

TABLE 1. Flow visualization of the wake of a cylinder vibrating in line with an incident uniform flow. Reynolds number $Re = 190$, Strouhal frequency $f_s = 36{\cdot}6$ Hz.

5. Flow visualization of the vortex street

The photographs referred to in this section were all taken at a Reynolds number of 190. The in-line vibration frequencies ranged from 64 to 81 Hz, or from $f/f_s = 1{\cdot}74$ to $2{\cdot}20$ for a Strouhal frequency $f_s = 36{\cdot}6$ Hz, and the amplitudes and frequencies at which the photographs were taken are listed in table 1. Except for the stationary-cylinder reference, figure 3 (plate 1), all the photographs were taken at amplitudes greater than those at which locking-on occurs.

5.1. *The effects of vibration frequency*

The photographs in figures 4(*a*)–(*c*) (plates 1 and 2) were taken over a range of frequencies between $f/f_s = 1{\cdot}76$ and $2{\cdot}20$. Under these conditions the cylinder was vibrating in line at a frequency near twice the Strouhal value and a single vortex was shed during each cycle of the cylinder's motion. The resulting form of the vortex wake is shown in the figures and may be compared with the stationary-cylinder wake in figure 3. There is a basic similarity between the two cases, with the street in each composed of vortices of opposite sign that were shed from alternate sides of the cylinder. Also, the frequency for vortices of like sign is half the in-line vibration frequency, or equivalently, the shedding frequency is near the Strouhal value and near the cross-flow locked-on range. The longitudinal spacing of the wake varies inversely with the frequency of the oscillation, and frequencies greater than twice the Strouhal frequency, for example $f/f_s = 2{\cdot}06$ and $2{\cdot}20$, result in reduction of the longitudinal spacing while frequencies less than twice the Strouhal frequency, as in figure 4(*a*), increase it (see also figure 6(*a*), plate 4, which was taken at $f/f_s = 1{\cdot}88$). The photographs shown in figure 4 were taken at different amplitudes of oscillation in order to ensure that the amplitude was greater than the locking-on threshold, which varied with frequency as shown in figure 2.

The in-line oscillations also reduce the transverse spacing of the vortex street, as can be seen from a comparison between figure 3 and any of figures 4(*a*)–(*c*). This behaviour is especially evident in figure 4(*a*), where the street almost appears to be a line of counter-rotating vortices with vanishing transverse spacing. For this case the cylinder is vibrating at an amplitude of $0{\cdot}22d$, which is well above the locking-on threshold at that frequency.

The photographs in figure 5(*a*) and (*b*) (plate 3) illustrate the second of the two fundamental vortex patterns which appeared as a result of the in-line vibrations. In this case two vortices were shed during each cycle of the cylinder's motion, thus resulting in a frequency for vortices of like sign near $2f_s$, or equivalently, a shedding frequency near twice the Strouhal frequency. The motion of the vortices after formation is very complex, but the photographs suggest that the early wake is arranged into alternating pairs of vortices with each pair being made up of vortices of opposite sign. This is to say, during one motion cycle at a frequency near twice the Strouhal value, two vortices are shed from alternate sides of the cylinder and form a vortex pair as they subsequently move downstream. The photographs also imply that one vortex of the pair is stronger, or of greater circulation, than the other.

Though the two photographs shown in figure 5 were taken at $f/f_s = 1{\cdot}74$ and $1{\cdot}92$, the same pattern of behaviour was also observed at $f/f_s \geqslant 2$ for amplitudes of oscillation above the locking-on threshold. The experiments in the present case were carried out at reduced velocities which overlap both of the instability regions in which vortex-induced oscillations occur in line with the flow, and in which both single vortices and pairs of vortices are shed during a cycle of the cylinder's motion (King *et al.* 1973). It should be noted that the two types of vortex shedding appeared singly in distinct ranges of U_r in the flow-induced vibration experiments reported by King *et al.*, but that the two patterns were observed intermittently over the entire range $U_r = 2{\cdot}1$–$4{\cdot}4$ of the present forced-body experiments.

5.2. *The effects of vibration amplitude*

When a cylinder vibrates in the cross-flow direction, it has been observed that increases in the amplitude of oscillation are accompanied by decreased lateral spacing of the vortex street (Koopmann 1967; Griffin & Votaw 1972; Griffin & Ramberg 1974). Similar behaviour is illustrated in the photographs of figures 6(*a*)–(*c*) (plates 4 and 5). In these experiments the cylinder was vibrated at a frequency of $69{\cdot}2$ Hz, or $f/f_s = 1{\cdot}88$, and at several amplitudes above the locking-on threshold. The first photograph was taken with the cylinder vibrating at $a = 0{\cdot}12d$ and the features of the vortex wake structure which are readily observed include a decrease in the lateral spacing compared with the corresponding stationary-cylinder wake and a lengthening of the longitudinal spacing relative to previous results at $f > 2f_s$ (see figures 4*b*, *c*). Again there is a single vortex shed during each cycle of the cylinder's motion, thus leading to a locked-on frequency of $\frac{1}{2}f$ near the Strouhal frequency f_s.

As the amplitude of vibration is increased to $a = 0{\cdot}15d$, there is no change in the longitudinal spacing but the lateral spacing of the street is decreased still further from its value in the wake of the stationary cylinder. The street in fact approaches once more the configuration resembling a line of counter-rotating vortices with very small lateral spacing. The amplitude of the in-line oscillations is only $0{\cdot}20d$ when the street spacing is reduced nearly to zero and the incipient stages of a secondary vortex formation are begun, as in figure 6 (*c*). Such behaviour has also been observed when a cylinder undergoes cross-flow oscillation (Griffin & Ramberg 1974). The secondary vortex formation becomes more apparent as the amplitude is increased even further as shown in figure 7 (plate 5), which was taken at $f/f_s = 1{\cdot}88$ and $a = 0{\cdot}24d$. During a cycle of the cylinder's motion only a single counter-clockwise vortex is shed, while two clockwise vortices are shed during alternate cycles. This wake pattern is not to be confused with either fundamental pattern just discussed. As will be shown, this particular pattern is solely a consequence of the vibration amplitude reaching a value too great to permit the previous alternating pattern to continue.

Tatsuno (1972) photographed three flow patterns at $a/d = 0{\cdot}54$ and at f/f_s between $1{\cdot}34$ and $1{\cdot}80$. This photographic study, though limited in extent, also gives some evidence of the existence at a Reynolds number of 100 of both the fundamental flow regimes as well as the asymmetric pattern associated with large amplitude cylinder motions.

6. Measurements of vortex spacing

The longitudinal spacing of the vortices in the wake was measured for the case in which a single vortex was shed during each cycle of the cylinder's vibration. The spacing measurements were made by simultaneously traversing the wake with the hot wire and flashing the strobes in the aerosol sheet in order to remove any doubt as to the type of flow regime which was present. Both qualitative measurements from the photographic negatives and quantitative measurements of the correlation between the vortices and the cylinder motion were made and compared. All of the data were obtained at various amplitudes above the locking-on threshold in order that the wake and the vibrations had a single characteristic frequency. As shown by the photographs discussed in §5, the amplitude of the oscillations had no effect on the longitudinal spacing.

A typical distribution of the correlation between the vortex signal and the cylinder-motion reference signal is shown in figure 8. The hot-wire probe was traversed downstream at a distance $y \approx 2d$ from the centre-line of the wake in order to preclude any interference in the recorded velocity signal from vortices of opposing sign. The cylinder-motion reference signal was of half the vibration frequency, since vortices of like sign were shed in this flow regime during every other cycle of the vibration. The resulting downstream correlogram then yielded the longitudinal spacing of vortices of the same sign, since the correlation function is a direct measurement of the phase between the two signals of identical frequencies. A similar method for measuring vortex spacing has been used by Twigge-Molecey & Baines (1973) and by Ramberg & Griffin (1976). In the latter paper it was shown that the downstream correlogram method yields the same result as would be obtained by directly measuring the phase angle between two signals as a function of downstream distance.

The results obtained are listed in table 2, and the measurements from the photographs are plotted in figure 9 together with a least-squares-fit line in order

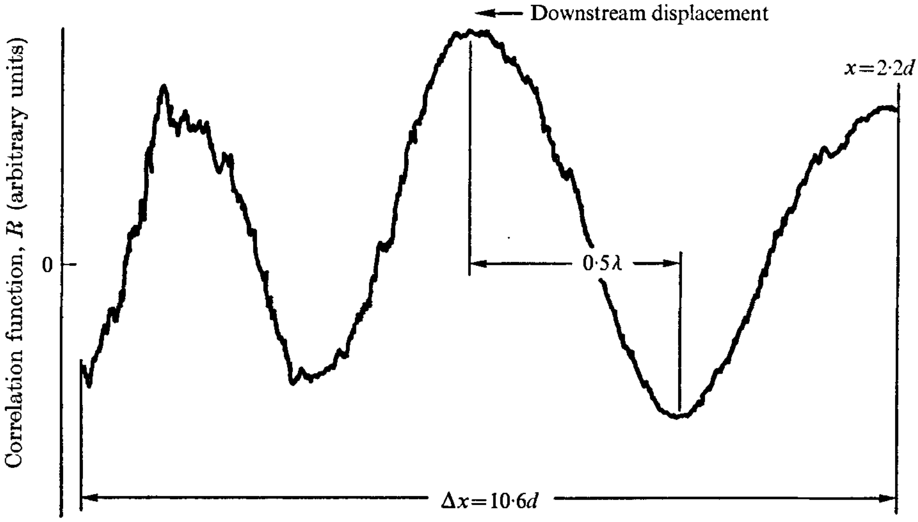

FIGURE 8. The correlation function R between a hot-wire signal in the cylinder wake and a cylinder-vibration reference signal. The hot wire, positioned at a transverse displacement $y \approx 2d$ from the centre-line of the wake, was traversed in the downstream direction from a cylinder vibrating in line with the incident flow at $Re = 190$. A single vortex was shed during each cycle of the cylinder's vibration. $f = 2f_s$, $a = 0\cdot09d$, $\lambda = 4\cdot9d$.

Vibration frequency f (Hz)	Frequency ratio f/f_s	Vortex spacing λ/d†	Vortex spacing λ_p‡	Relative change $\Delta\lambda/\lambda$	Vortex convection speed, $\frac{1}{2}f\lambda/U$
		Reynolds number Re = 190			
69·2	1·88	—	167	+0·07	0·94
73·6	2·00	4·9	155·7§	0	0·93
75·6	2·06	—	148	−0·05	0·91
78·9	2·14	4·7	—	−0·04	0·96
80·4	2·18	—	142	−0·09	0·92
		Reynolds number Re = 100, $a/d = 0\cdot54$			
	1·38*	8·8*	—	+0·47‖	0·88‖
	1·72	7·2	—	+0·20	0·90
	2·00	6·0	—	0	0·90
	2·20	5·4	—	−0·10	0·86

† From wake correlograms (see figure 8).
‡ Arbitrary scale; one unit = 5 mm on the screen of the photo enlarger.
§ Least-squares estimate.
* From Tatsuno (1972); one vortex was shed during each cycle of the cylinder's oscillation in water.
‖ Computed from the results of Tatsuno.

TABLE 2. Longitudinal vortex spacing in the wake of a cylinder vibrating in line with an incident uniform flow. Strouhal frequency $f_s = 36\cdot6$ Hz.

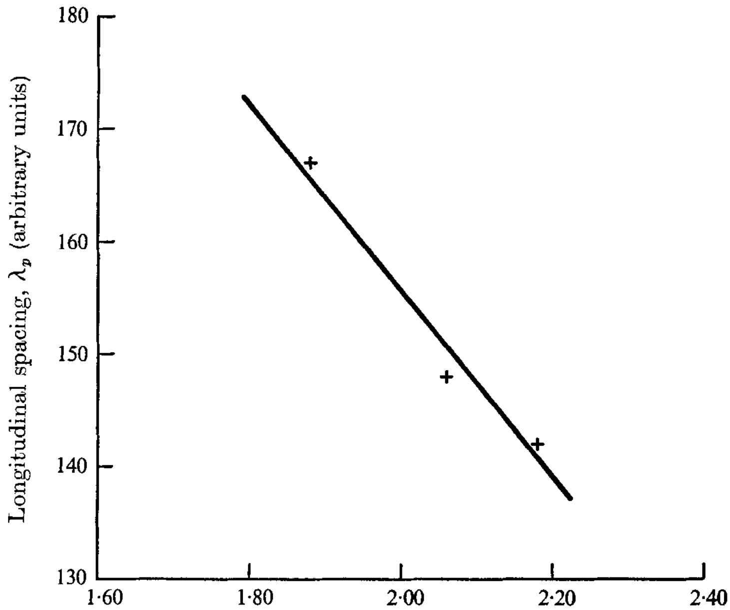

FIGURE 9. The longitudinal vortex spacing λ_p, measured from photographic negatives, as a function of in-line vibration frequency f/f_s. +, photographic measurements; ——, fitted straight line, $\lambda_p = 322{\cdot}50 + 84{\cdot}41 f/f_s$.

to determine a correspondence between the two measurement procedures. Once this correspondence is found, as indicated in table 2, it becomes a simple matter to compute the changes in spacing and to determine the convection speed of the vortex centres. The results again show the vortex spacing to be inversely proportional to the vibration frequency, with frequencies greater than twice the Strouhal frequency resulting in decreased spacing and vice versa. The vortex spacing λ in the wake when the cylinder is vibrating in line with the flow at twice the Strouhal frequency is equal to the spacing behind the stationary cylinder at the same Reynolds number when the flow regime behind the vibrating cylinder is of the type shown in figures 4 and 6.

The changes in longitudinal spacing from Tatsuno (1972) listed in table 2 are in good agreement with those of the present study. At the lower Reynolds number of 100 in water, λ was also found to be inversely dependent on the vibration frequency, as shown by the relative change in the measured spacings. The convection speed of the vortices remains nearly constant and for each of the two experiments the values given are typical of the alternating vortex patterns shown in figures 3, 4 and 6.

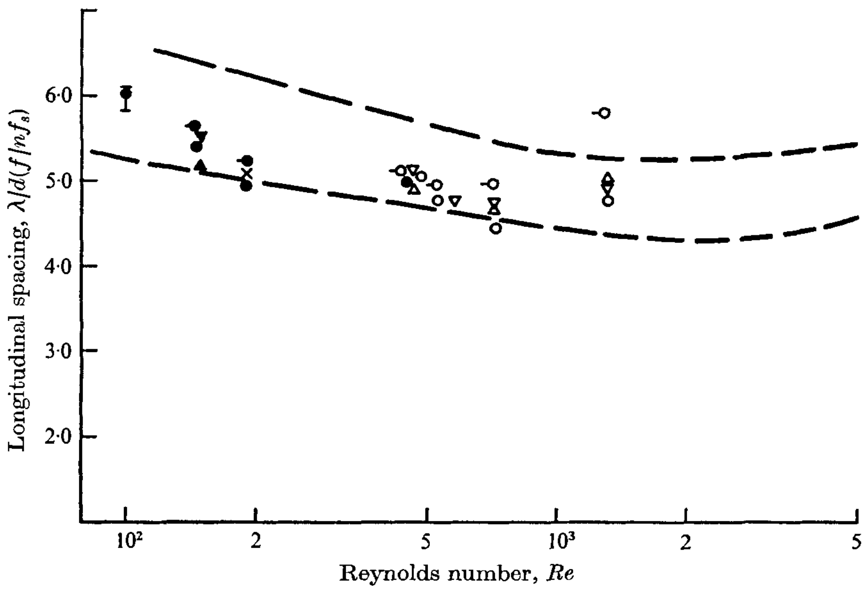

FIGURE 10. Longitudinal vortex spacing $\lambda/d(f/nf_s)$ and reciprocal Strouhal number St^{-1} as a function of Reynolds number Re. All of the measurements were made in the wakes of vibrating cylinders and cables. ○, $f/nf_s = 1$; △, $f/nf_s = 0{\cdot}9$; ×, $f/nf_s = 1{\cdot}07$; ▽, $f/nf_s = 1{\cdot}1$; ⧲, $f/nf_s = 0{\cdot}69$–$1{\cdot}10$ (Tatsuno 1972); -○, St^{-1}. Dashed lines denote bounds of St^{-1} for smooth (lower) and rough (upper) circular cylinders. Open symbols refer to vibrating cables, closed symbols to vibrating cylinders. Data points at $Re = 100$ and $Re = 190$ correspond to in-line vibration ($n = 2$); all other data correspond to cross-flow vibration ($n = 1$).

7. A comparison between in-line and transverse oscillations of bluff bodies

The in-line vibration experiments just discussed and other recent cross-flow vibration experiments at similar Reynolds numbers (see, in part, Griffin & Ramberg 1974, 1975) make possible a straightforward comparison between the two cases. This comparison will necessarily relate to the particular case of a vortex street with a shedding frequency near the Strouhal value f_s (i.e. figures 4 and 6) since this flow regime exists for both in-line and cross-flow vibrations of the cylinder.

The most obvious similarities lie in the effects of vibration amplitude and frequency on the vortex spacing behind the cylinder. The longitudinal spacing λ varies inversely with frequency in each case, with frequencies of oscillation greater than the Strouhal frequency f_s or twice f_s producing contraction of the longitudinal spacing and vice versa. As shown in the preceding section for the in-line case and in a recent paper (Griffin & Ramberg 1974) for the cross-flow case, the longitudinal spacing remains at the stationary-cylinder value when the cylinder is vibrated at f_s or $2f_s$ for cross-flow or in-line oscillations, respectively, at the same Reynolds number.

The longitudinal spacing λ is plotted in figure 10 as a function of the Reynolds number. All of the results except those at $Re = 100$ were obtained at NRL from measurements in the wakes of both stationary and vibrating cylinders and cables at Reynolds numbers up to 1500. The measurements made at $Re = 100$ and $Re = 190$ with the cylinder vibrating in line compare well with the measurements made for cross-flow oscillations. The flagged points represent the experimental values of St^{-1} since

$$\frac{\lambda}{d}\left(\frac{f}{nf_s}\right) = \frac{U_\phi}{U}St^{-1},$$

where U_ϕ is the convection speed of the vortex centres and where $n = 1$ and 2 for cross-flow and in-line vibrations respectively. The values of U_ϕ reported in the preceding section for the in-line vibrations are also in good agreement with those obtained at the other Reynolds numbers. These measurements of U_ϕ for the cross-flow experiments between $Re = 100$ and 1500 fall in a range of U_ϕ of 0·80–0·96 with the lower values of U_ϕ found at the highest Reynolds number, $Re = 1300$, in figure 10 (see Ramberg & Griffin 1976).

Another direct correspondence between the two vibration regimes concerns the effects of vibration amplitude upon the vortex street: an increase in the amplitude of oscillation produces a decrease in the transverse spacing of the vortex street. It is interesting to note that the transverse spacing becomes vanishingly small under the influence of cross-flow oscillations at $a = 0{\cdot}8$–$1{\cdot}3d$, depending on the frequency, whereas for the in-line oscillations discussed in previous sections the street becomes almost collinear at amplitudes of only 0·15–0·20d.

In conjunction with the decreased transverse spacing the vortex-street geometry has been observed to undergo a change at large cross-flow amplitudes of oscillation. Such a transition is shown in figure 7 for the case when the cylinder is vibrating in line with the flow at $f/f_s = 1{\cdot}88$ and $a = 0{\cdot}23d$. There are three vortices shed during a cycle of the motion, two being clockwise and one counter-clockwise. During cross-flow oscillations two counter-clockwise vortices and a single clockwise vortex were shed during each cycle of the motion, but otherwise the two flow fields are similar.

It appears that the initiation of the secondary vortices in figure 7 is related to the limit $h/\lambda \to 0$, as previously shown for the case of cross-flow oscillations (Griffin & Ramberg 1974). This limit $h/\lambda = 0$ coincides with the transition from a drag- to a thrust-type street of vortices where the induced vortex velocities and fluid forces on the cylinder parallel to the flow change sign. Again there appears in the case of the in-line vibrations to be a shift to the asymmetric geometry of figure 7 in order to preclude the development of a thrust-type vortex street as the cylinder amplitude is increased beyond a critical value corresponding to zero lateral spacing. It is also possible to observe once again the 'fission' of the finite vortex street as the transverse spacing becomes vanishingly small. This fission or breakup of a finite vortex pattern was generated in the computer experiments of Christiansen & Zabusky (1973) and observed in the authors' prior cross-flow vibration experiments. The onset of this process is visible in the flow pattern downstream in figure 6 (*b*) and is more pronounced in the downstream portion of the asymmetric pattern shown in figure 7.

8. Summary and concluding remarks

The aim of this programme was to measure the bounds of the regime in which vibrations of a cylinder in line with an incident flow control the vortex shedding and cause the wake and cylinder frequencies to lock on or synchronize together. Measurements were also made of the vortex patterns and spacing by means of both hot-wire surveys and flow visualization.

When a circular cylinder is forced to undergo vibrations in line with an incident flow, the vortex shedding locks on to the vibration frequency over a range of frequencies from 120 to 250 % of the Strouhal frequency f_s. The amplitude threshold at which the locking-on is initiated decreases from 30 % of a diameter to about 7 % as the vibration frequency increases from $1{\cdot}2f_s$ to $2f_s$. As the frequency is increased to $2{\cdot}5f_s$ the threshold of the locking-on increases to about 12–15 % of a diameter.

These synchronized in-line oscillations correspond to a range of reduced velocities $U_r = U/fd$ between 2·1 and 4·4, where U is the incident flow speed, f is the forced vibration frequency and d is the cylinder's diameter. In-line vortex-induced oscillations of model and prototype cylinders have been observed to occur within the range $U_r = 1{\cdot}5$–$4{\cdot}0$.

Two distinct forms of vortex street were observed when the cylinder was vibrated in line with the flow. The first of these, call it regime I, is characterized by the shedding of two vortices of opposing sign during each cycle of the cylinder's motion at a frequency f near twice the Strouhal frequency f_s. The resulting pattern is very complex and has a frequency f for vortices of like sign, but the near wake can be characterized generally as an alternating street of vortex pairs with each pair made up of two vortices of opposing rotation.

The second form of street, regime II, is characterized by the shedding of a single vortex during each cycle of the motion. The resulting street has a frequency of $\frac{1}{2}f$ for vortices of like sign, where again f is the vibration frequency. Flow regime II shares many of the characteristics which have been observed when cylinders have been forced to oscillate in the cross-flow direction. Among these is an inverse dependence of the longitudinal vortex spacing on the vibration frequency. The longitudinal spacing decreased from 107 to 90 % of the spacing at $2f_s$ as the vibration frequency increased from $1{\cdot}88f_s$ to $2{\cdot}2f_s$. Also, when a cylinder vibrated in line at twice the Strouhal frequency, the longitudinal spacing for regime II was equal to the longitudinal spacing behind a stationary cylinder and behind a cylinder which vibrated transverse to the flow at the Strouhal frequency.

The transverse spacing of the vortices in regime II shows a similar dependence on in-line vibration amplitude to that found for cylinders vibrating in cross-flow. As the amplitude is increased, the transverse spacing decreases until, in the limit of vanishing transverse spacing, the wake geometry passes from an alternating street of vortices to an unusual street where three vortices are formed during any two successive cycles of the cylinder motion at vibration frequencies near $2f_s$. This secondary vortex formation had previously been observed to occur at cross-flow amplitudes of $0{\cdot}8$–$1{\cdot}3d$, whereas for in-line oscillations the transverse spacing of the street became vanishingly small at amplitudes of only 0·15–0·25d.

'Vortex fission' was observed as a vortex street of vanishingly small transverse spacing was generated by vibrating the cylinder in line with the flow. This phenomenon had previously been observed in computer experiments with collinear patterns of vortices of alternating sign (Christiansen & Zabusky 1973) and when vortex streets with vanishing transverse spacing were generated by cross-flow vibrations of a cylinder (Griffin & Ramberg 1974).

The authors wish to acknowledge the support of the Naval Research Laboratory for this programme of experiments, and to thank the NRL Photography Branch for the careful preparation of the flow-visualization photographs and negatives. The authors also wish to thank Prof. H. Honji of Kyushu University for providing them with a copy of the report by Tatsuno.

REFERENCES

BERGER, E. W. & WILLE, R. 1972 *Ann. Rev. Fluid Mech.* **4**, 313–340.

CHRISTIANSEN, J. P. & ZABUSKY, N. 1973 *J. Fluid Mech.* **61**, 219–243.

GRIFFIN, O. M. 1971 *Trans. A.S.M.E., J. Appl. Mech.* **38**, 729–738.

GRIFFIN, O. M. & RAMBERG, S. E. 1974 *J. Fluid Mech.* **66**, 553–576.

GRIFFIN, O. M. & RAMBERG, S. E. 1975 *J. Fluid Mech.* **69**, 721–729.

GRIFFIN, O. M., RAMBERG, S. E., VOTAW, C. W. & KELLEHER, M. D. 1973 *Proc. Int. Cong. Instrumentation in Aerospace Simulation Facilities* (*IEEE*), pp. 133–139.

GRIFFIN, O. M., SKOP, R. A. & RAMBERG, S. E. 1975 *Offshore Tech. Conf., Houston*, paper OTC 2319.

GRIFFIN, O. M. & VOTAW, C. W. 1972 *J. Fluid Mech.* **55**, 31–48.

KING, R. 1974 *Offshore Tech. Conf., Houston*, paper OTC 1948.

KING, R., PROSSER, M. J. & JOHNS, D. J. 1973 *J. Sound Vib.* **29**, 169–188.

KOOPMANN, G. H. 1967 *J. Fluid Mech.* **28**, 501–512.

MAIR, W. A. & MAULL, D. J. 1971 *J. Fluid Mech.* **45**, 209–224.

NAUDASCHER, E. (ed.) 1974 *Flow-Induced Structural Vibrations*, pp. 587–601. Springer.

PARKINSON, G. V. 1971 *Phil. Trans.* A **229**, 395–409.

RAMBERG, S. E. & GRIFFIN, O. M. 1976 *Trans. A.S.M.E., J. Fluids Engng*, **98**, 10–18.

SAINSBURY, R. & KING, N. 1971 *Proc. Inst. Civil Engrs*, **49**, 269–302.

TANIDA, Y., OKAJIMA, A. & WATANABE, Y. 1973 *J. Fluid Mech.* **61**, 769–784.

TATSUNO, M. 1972 *Bull. Res. Inst. Appl. Mech., Kyushu University*, **36**, 25–37 (in Japanese).

TWIGGE-MOLECEY, C. F. M. & BAINES, W. D. 1973 *Proc. A.S.C.E., J. Engng Mech.* **99**, 803–818.

WOOTTON, L. R., WARNER, M. H., SAINSBURY, R. N. & COOPER, D. H. 1972 *Construction Indust. Res. & Inf. Ass. Lond. Rep.* CIRIA 41.

FIGURE 3. Flow visualization of the wake of a stationary cylinder at a Reynolds number of 190. Strouhal frequency f_s = 36·6 Hz, cylinder diameter d = 4 mm, Strouhal number = 0·19.

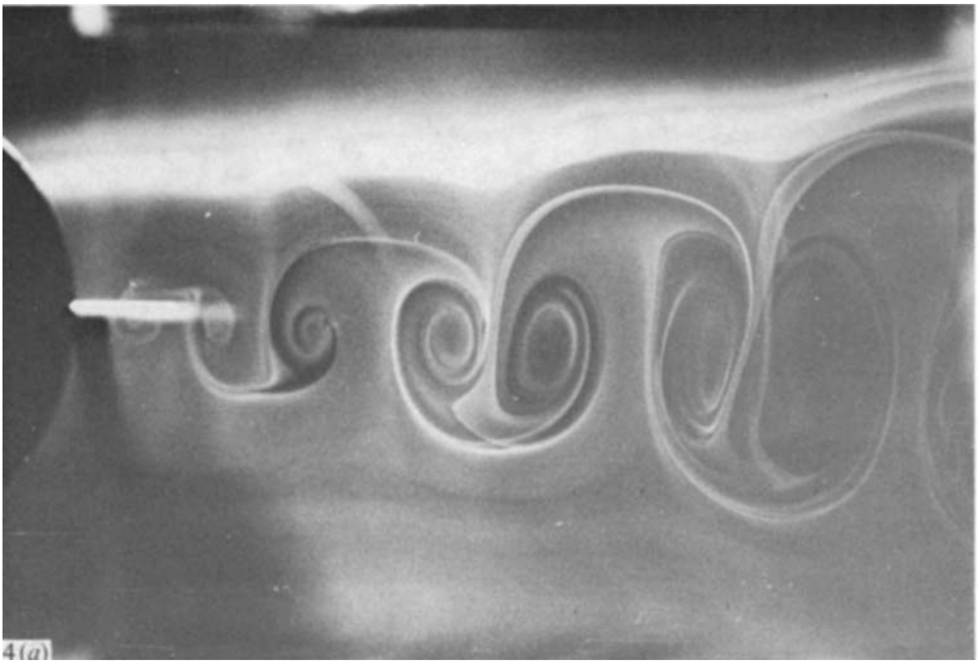

FIGURE 4(a). For legend see plate 2.

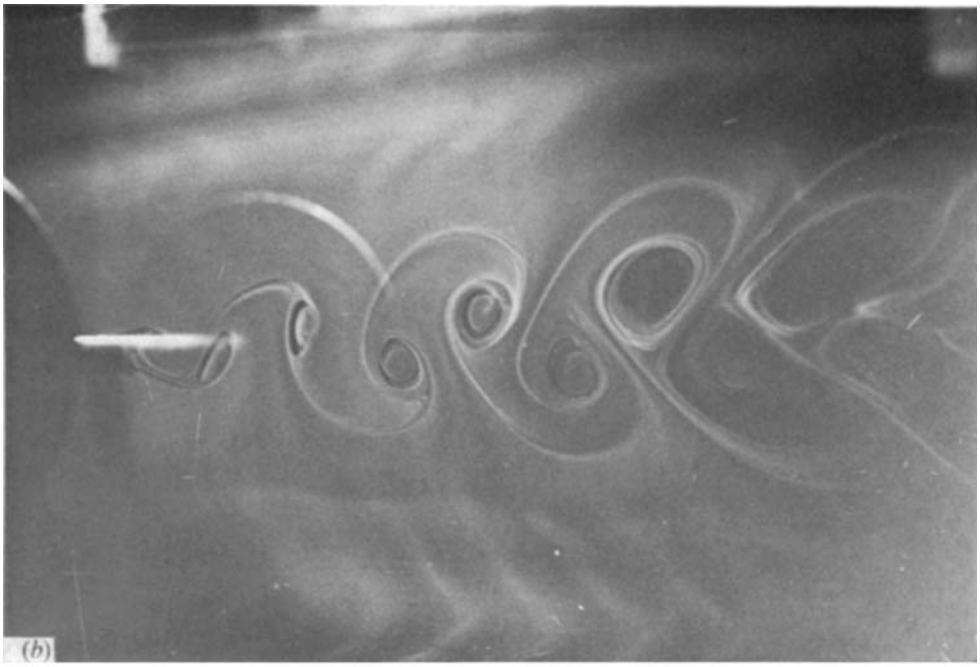

FIGURE 4. The effects of frequency on the vortex wake of a cylinder vibrating in line with an incident flow at a Reynolds number of 190. A single vortex was shed during each cycle of the cylinder's vibration. (*a*) $f/f_s = 1{\cdot}76$, (*b*) $f/f_s = 2{\cdot}06$, (*c*) $f/f_s = 2{\cdot}20$.

FIGURE 5. Vortex shedding from a cylinder vibrating in line with an incident flow at a Reynolds number of 190. Two vortices were shed during each cycle of the cylinder's vibration. (*a*) $f/f_s = 1{\cdot}74$, (*b*) $f/f_s = 1{\cdot}92$.

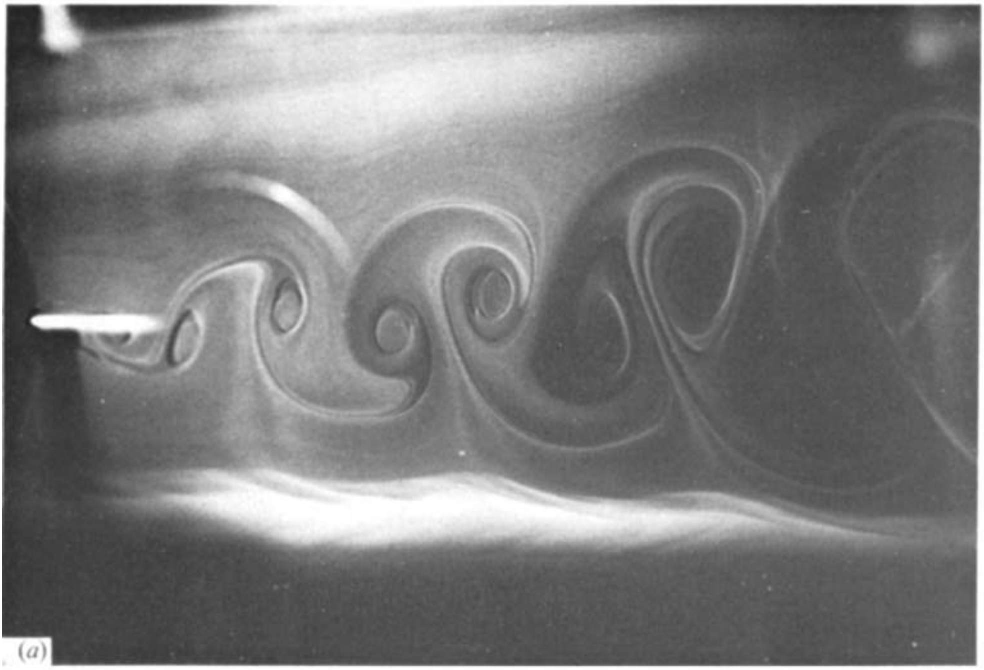

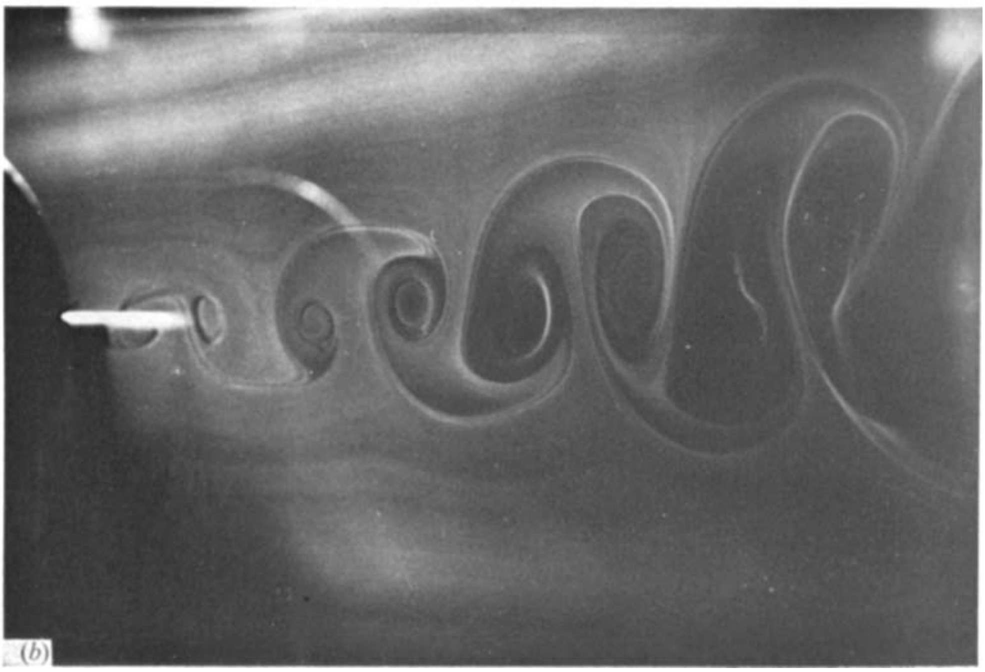

FIGURES 6 (a, b). For legend see plate 5.

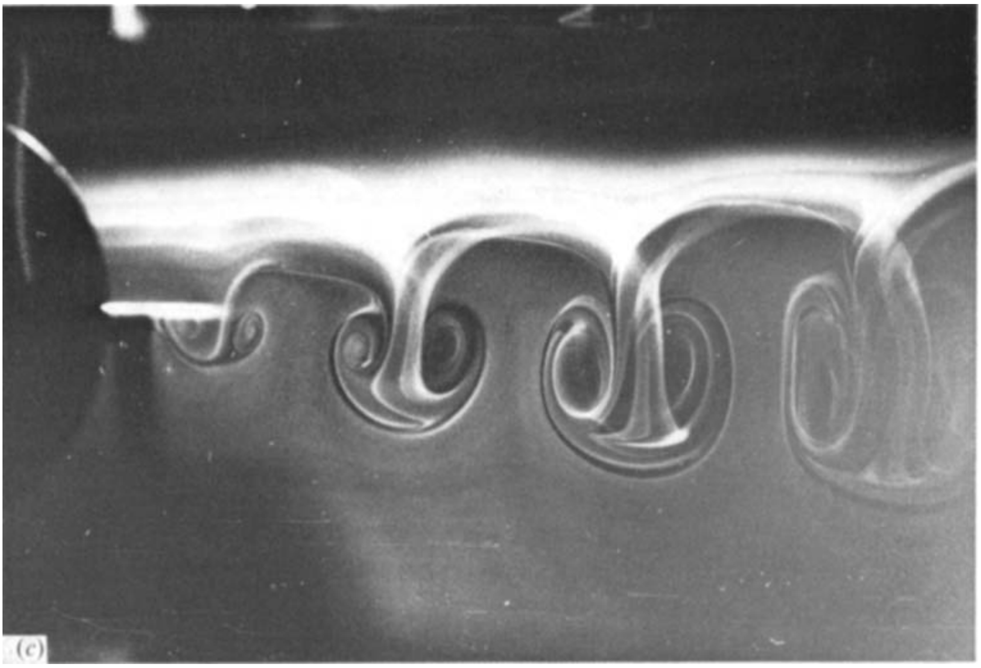

FIGURE 6. The effects of vibration amplitude on the wake of a cylinder vibrating in line with an incident flow at a Reynolds number of 190. A single vortex was shed during each cycle of the cylinder's vibration at a frequency of $f/f_s = 1{\cdot}88$. (*a*) $a = 0{\cdot}12d$, (*b*) $a = 0{\cdot}15d$, (*c*) $a = 0{\cdot}20d$.

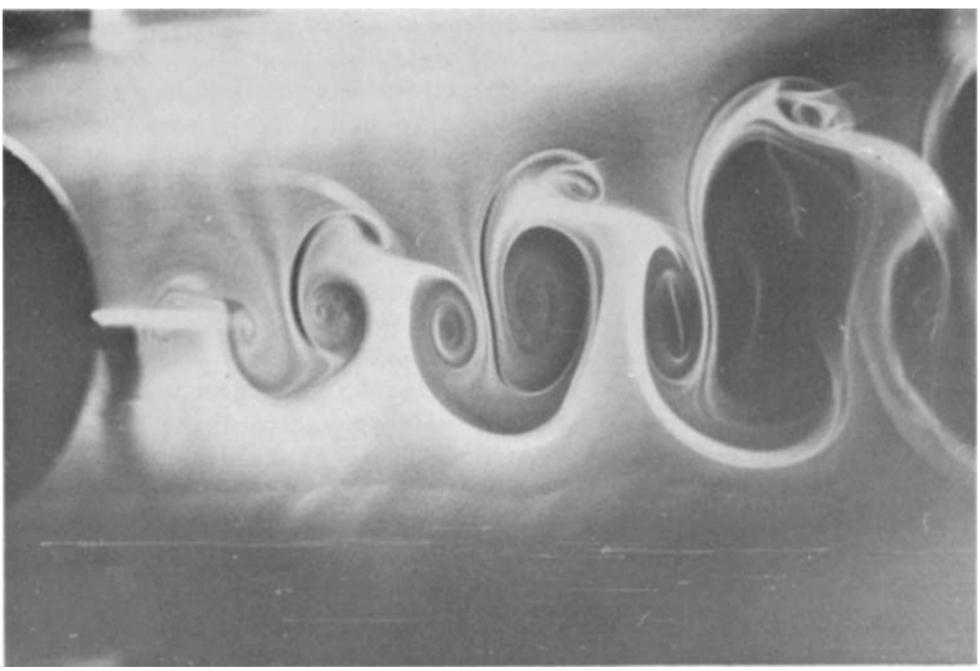

FIGURE 7. Secondary vortex formation in the wake of a cylinder vibrating in line with an incident flow at a Reynolds number of 190. $f/f_s = 1{\cdot}88$, $a = 0{\cdot}24d$.